

Measurement of the Decay $K_L \rightarrow \pi^0 \gamma \gamma$

A. Alavi-Harati,¹² I. F. Albuquerque,¹⁰ T. Alexopoulos,¹² M. Arenton,¹¹ K. Arisaka,² S. Averitte,¹⁰ A. R. Barker,⁵ L. Bellantoni,⁷ A. Bellavance,⁹ J. Belz,¹⁰ R. Ben-David,⁷ D. R. Bergman,¹⁰ E. Blucher,⁴ G. J. Bock,⁷ C. Bown,⁴ S. Bright,⁴ E. Cheu,^{1,*} S. Childress,⁷ R. Coleman,⁷ M. D. Corcoran,⁹ G. Corti,¹¹ B. Cox,¹¹ M. B. Crisler,⁷ A. R. Erwin,¹² R. Ford,⁷ A. Golossanov,¹¹ G. Graham,⁴ J. Graham,⁴ K. Hagan,¹¹ E. Halkiadakis,¹⁰ K. Hanagaki,⁸ S. Hidaka,⁸ Y. B. Hsiung,⁷ V. Jejer,¹¹ J. Jennings,² D. A. Jensen,⁷ R. Kessler,⁴ H. G. E. Kobrak,³ J. LaDue,⁵ A. Lath,¹⁰ A. Ledovskoy,¹¹ P. L. McBride,⁷ A. P. McManus,¹¹ P. Mikelsons,⁵ E. Monnier,^{4,†} T. Nakaya,⁷ U. Nauenberg,⁵ K. S. Nelson,¹¹ H. Nguyen,⁷ V. O'Dell,⁷ M. Pang,⁷ R. Pordes,⁷ V. Prasad,⁴ C. Qiao,⁴ B. Quinn,⁴ E. J. Ramberg,⁷ R. E. Ray,⁷ A. Roodman,⁴ M. Sadamoto,⁸ S. Schnetzer,¹⁰ K. Senyo,⁸ P. Shanahan,⁷ P. S. Shawhan,⁴ W. Slater,² N. Solomey,⁴ S. V. Somalwar,¹⁰ R. L. Stone,¹⁰ I. Suzuki,⁸ E. C. Swallow,^{4,6} R. A. Swanson,³ S. A. Taegar,¹ R. J. Tesarek,¹⁰ G. B. Thomson,¹⁰ P. A. Toale,⁵ A. Tripathi,² R. Tschirhart,⁷ Y. W. Wah,⁴ J. Wang,¹ H. B. White,⁷ J. Whitmore,⁷ B. Winstein,⁴ R. Winston,⁴ J.-Y. Wu,⁵ T. Yamanaka,⁸ and E. D. Zimmerman⁴

(KTeV Collaboration)

¹University of Arizona, Tucson, Arizona 85721

²University of California at Los Angeles, Los Angeles, California 90095

³University of California at San Diego, La Jolla, California 92093

⁴The Enrico Fermi Institute, The University of Chicago, Chicago, Illinois 60637

⁵University of Colorado, Boulder, Colorado 80309

⁶Elmhurst College, Elmhurst, Illinois 60126

⁷Fermi National Accelerator Laboratory, Batavia, Illinois 60510

⁸Osaka University, Toyonaka, Osaka 560, Japan

⁹Rice University, Houston, Texas 77005

¹⁰Rutgers University, Piscataway, New Jersey 08855

¹¹The Department of Physics and the Institute of Nuclear and Particle Physics, University of Virginia, Charlottesville, Virginia 22901

¹²University of Wisconsin, Madison, Wisconsin 53706

(Received 22 February 1999)

We report on a new measurement of the decay $K_L \rightarrow \pi^0 \gamma \gamma$ by the KTeV experiment at Fermilab. We determine the $K_L \rightarrow \pi^0 \gamma \gamma$ branching ratio to be $(1.68 \pm 0.07 \pm 0.08) \times 10^{-6}$. Our data show the first evidence for a low-mass $\gamma \gamma$ signal as predicted by recent $\mathcal{O}(p^6)$ chiral perturbation calculations which include vector meson exchange contributions. From our data, we extract a value for the effective vector coupling $a_V = -0.72 \pm 0.05 \pm 0.06$.

PACS numbers: 13.20.Eb, 11.30.Er, 12.39.Fe, 13.40.Gp

Studying the decay $K_L \rightarrow \pi^0 \gamma \gamma$ is important for understanding the low energy hadron dynamics of chiral perturbation theory. Because of the high backgrounds associated with this decay, the first measurement of the $K_L \rightarrow \pi^0 \gamma \gamma$ branching ratio [1] was performed only relatively recently. Other measurements soon confirmed this result [2,3] with the measured branching ratio [4], $(1.70 \pm 0.28) \times 10^{-6}$, approximately 3 times higher than the predictions from $\mathcal{O}(p^4)$ chiral perturbation calculations [5]. More recent calculations [6–9] which include $\mathcal{O}(p^6)$ corrections and vector meson exchange contributions obtain a branching ratio consistent with the measured value.

The rate for $K_L \rightarrow \pi^0 \gamma \gamma$ can be expressed in terms of two independent Lorentz invariant amplitudes which represent $J = 0$ and $J = 2$ two-photon states. The contributions of the two amplitudes are determined by two Dalitz parameters, $z = (m_{34}/m_K)^2$ and $y = |E_3 - E_4|/m_K$, where E_3 and E_4 are the energies of the non- π^0 photons in the kaon center of mass frame and m_{34} is their invariant

mass. Vector meson exchange contributions to the amplitudes are parametrized by an effective coupling constant a_V [9], and the z and y Dalitz variables are sensitive to the value of a_V as shown in Fig. 1. In particular, certain values of a_V result in a sizeable low-mass tail in the m_{34} distribution. Because of limited statistics, previous measurements were not sensitive to such a low-mass tail. With a sufficiently large event sample, it is possible to test the predictions of $\mathcal{O}(p^6)$ chiral perturbation theory with vector meson contributions and to precisely determine the parameter a_V directly from the data. A precise determination of a_V also allows one to predict the relative contributions of the CP -conserving and direct CP -violating components of $K_L \rightarrow \pi^0 e^+ e^-$ which can proceed through the CP -conserving process $K_L \rightarrow \pi^0 \gamma^* \gamma^* \rightarrow \pi^0 e^+ e^-$.

We recorded $K_L \rightarrow \pi^0 \gamma \gamma$ events using the KTeV detector located at Fermilab. Figure 2 shows a plan view of the detector as it was configured for the E832 experiment.

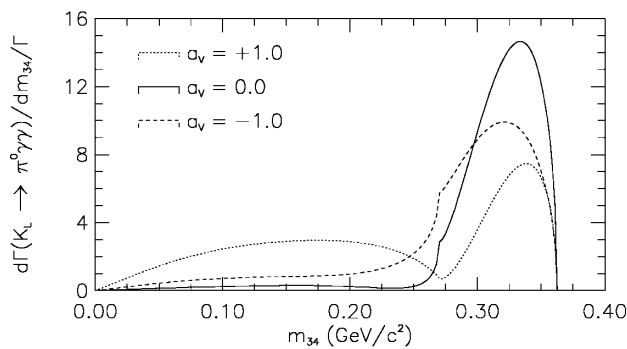


FIG. 1. Theoretical predictions for m_{34} for various values of a_V .

The main goal of the E832 experiment is to search for direct CP violation in $K \rightarrow \pi\pi$ decays. The $K_L \rightarrow \pi^0\gamma\gamma$ analysis utilizes the data set collected by the KTeV experiment during 1996 and 1997 for the direct CP violation search. Neutral kaons are produced in interactions of 800 GeV/ c protons with a beryllium oxide target. The resulting particles pass through a series of collimators to produce two nearly parallel beams. The beams also pass through lead and beryllium absorbers to reduce the fraction of photons and neutrons in each beam. Charged particles are removed from the beams by sweeping magnets located downstream of the collimators. To allow the K_S component to decay away, the decay volume begins approximately 94 m downstream of the target. In this experiment we have two simultaneous beams, one where the initial beam strikes a regenerator composed of a plastic scintillator and one that continues in vacuum. For this analysis, we consider only decays that originate in the beam opposite the regenerator, located 125 m downstream of the target.

The most critical detector elements for this analysis are a pure CsI electromagnetic calorimeter [10] and a hermetic lead-scintillator photon veto system. The CsI calorimeter is composed of 3100 blocks in a 1.9 by 1.9 m array that is 27 radiation lengths deep. Two 15 by 15 cm holes are located near the center of the array for the passage of the

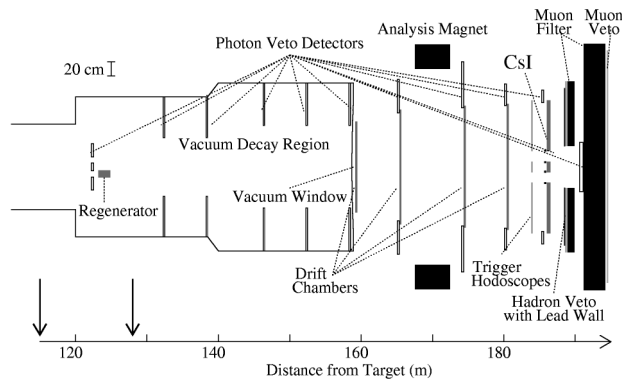


FIG. 2. Plan view of the KTeV detector as configured for the E832 experiment. The arrows indicate the decay region considered for this analysis.

two neutral beams. For electrons with energies between 2 and 60 GeV, the calorimeter energy resolution is below 1% and the nonlinearity is less than 0.5%. The position resolution of the calorimeter is approximately 1 mm. The spectrometer is surrounded by 10 detectors that veto photons at angles greater than 100 mrad. The first five vetoes consist of 16 lead-scintillator layers with 0.5 radiation length lead sampling followed by eight layers with 1.0 radiation length sampling. The other five vetoes have 32 layers with 0.5 radiation length sampling. The most upstream photon veto is located just upstream of the regenerator. This module has two beam holes and suppresses upstream decays. The remaining nine vetoes are arrayed along the length of the detector as shown in Fig. 2. On the face of the CsI calorimeter sits a tungsten-scintillator module that covers the inner half of the CsI blocks surrounding the beam holes. A final photon veto consists of three modules, each 10 radiation lengths thick, and sits behind the CsI calorimeter, covering the beam holes. This photon veto is used to reject events in which photons travel down either of the two beam holes in the calorimeter.

The KTeV detector also contains a spectrometer for reconstructing charged tracks. For this analysis, it is used to calibrate the CsI calorimeter using electrons from $K_L \rightarrow \pi^\pm e^\mp \nu$ decays, and to veto events with charged particles. This spectrometer consists of four planes of drift chambers, two located upstream and two downstream of an analyzing magnet with a transverse momentum kick of 0.4 GeV/ c . Downstream of the CsI calorimeter, there is a 10 cm lead wall, followed by a hodoscope (hadron-veto) used to reject hadrons hitting the calorimeter.

$K_L \rightarrow \pi^0\gamma\gamma$ events are recorded if they satisfy certain trigger requirements. The event must deposit greater than approximately 27 GeV in the CsI calorimeter and deposit no more than 0.5 GeV in the photon vetoes downstream of the vacuum window located at 159 m downstream of the target. The trigger includes a hardware cluster processor [11] that counts the number of clusters of contiguous blocks with energies above 1 GeV. The total number of clusters is required to be exactly four. These trigger requirements also select $K_L \rightarrow \pi^0\pi^0$ events that we use as normalization for the $K_L \rightarrow \pi^0\gamma\gamma$ events.

Reconstructing $K_L \rightarrow \pi^0\gamma\gamma$ events is difficult since there are few kinematical constraints giving rise to large backgrounds. In particular, $K_L \rightarrow \pi^0\pi^0$ and $K_L \rightarrow \pi^0\pi^0\pi^0$ decays, and hadronic interactions with material in the beam constitute the largest sources of background. Backgrounds resulting from kaon decays with charged particles are easily removed by discarding events with a large number of hits in the spectrometer.

In the offline analysis, we require exactly four reconstructed clusters of energy greater than 2.0 GeV while rejecting events with additional clusters above 0.6 GeV. Events with photons below 0.6 GeV do not contribute significantly to the background. The total kaon energy is required to be between 40 and 160 GeV. Using the

reconstructed energies and positions of the four clusters, we calculate the kaon decay position, assuming that all four photons result from the decay of a kaon. This position is then used to reconstruct a π^0 from the six possible $\gamma\gamma$ pairings. We choose the $\gamma\gamma$ pair whose reconstructed mass is closest to the nominal π^0 mass and require that $|m_{12} - m_{\pi^0}| < 3.0 \text{ MeV}/c^2$. The π^0 mass resolution is $0.84 \text{ MeV}/c^2$.

To remove $K_L \rightarrow \pi^0\pi^0$ decays we require the mass m_{34} be greater than $0.16 \text{ GeV}/c^2$ or less than $0.10 \text{ GeV}/c^2$. We cut asymmetrically about the π^0 mass to remove events with misreconstructed photons near the calorimeter beam holes. These events are well simulated by our Monte Carlo (MC) and only extend down to $0.10 \text{ GeV}/c^2$. Since we use the best π^0 mass to choose among the six possible $\gamma\gamma$ combinations, mispaired $K_L \rightarrow \pi^0\pi^0$ events constitute a possible background. There are three different ways to pair four photons to form $\pi^0\pi^0$ combinations. We remove mispaired $K_L \rightarrow \pi^0\pi^0$ events by reconstructing the other two $\pi^0\pi^0$ pairings and discarding events that have two $\gamma\gamma$ combinations near the π^0 mass. This cut removes 1.25% of the $K_L \rightarrow \pi^0\pi^0$ events in both the data and our Monte Carlo.

The hadronic interaction background results from neutrons in the beam interacting with material, primarily the vacuum window and the drift chambers. Such interactions produce $\pi^0\pi^0$ and $\pi^0\eta$ pairs. These events are not removed by the $2\pi^0$ cuts because the assumption that the invariant mass is m_K is incorrect in this case. To remove these events, we calculate the decay vertex of the six $\gamma\gamma$ combinations assuming that two of the photons result from a π^0 decay. Using this decay vertex, we reconstruct the mass of the other $\gamma\gamma$ pair and reject the event if the decay vertex of this $\gamma\gamma$ pair reconstructs downstream of 158 m and if the mass of that pair is within $15 \text{ MeV}/c^2$ of the known π^0 or η mass. We also require little activity in the hadron-veto to remove vacuum window interaction events that send hadrons into the CsI calorimeter.

$K_L \rightarrow \pi^0\pi^0\pi^0$ decays are the most difficult source of background to suppress in this analysis. These events can contribute to the background primarily through the following three mechanisms: (a) four photons hit the calorimeter (zero fusion), (b) five photons hit the calorimeter with two overlapping or fusing together to produce one cluster (single fusion), and (c) all six photons hit the calorimeter and four photons fuse together to reconstruct as two photons (double fusion). To reduce backgrounds from $K_L \rightarrow \pi^0\pi^0\pi^0$ events with zero and single fusions, we require little activity in the photon veto detectors. These criteria are determined from the amount of accidental activity in each counter and the response of each counter to photons from $3\pi^0$ events. For $K_L \rightarrow \pi^0\pi^0\pi^0$ events in which five or fewer photons hit the calorimeter, the reconstructed decay vertex lies downstream of the actual decay position. To remove these events, we require that the decay vertex be between 115 and 128 m downstream of the

target, as shown in Fig. 2. To further reduce the number of events with missing energy, we require that the center of energy of the four photons lie within a $10 \times 10 \text{ cm}^2$ region centered on one of the beam holes in the CsI calorimeter. The background from $3\pi^0$ events with only four photons in the calorimeter is below 0.5% of the expected signal level after these cuts.

The remaining $3\pi^0$ background results from events in which two or more photons fuse together in the CsI calorimeter. This background can be reduced by calculating a shape χ^2 for the energy deposited within the central three-by-three array of CsI blocks of a cluster compared to the energy distribution for a single photon. Clusters from a single photon will have a low χ^2 , whereas hadronic showers and fused clusters will usually result in a large χ^2 . Figure 3 shows the distribution of the maximum shape χ^2 variable of the four photons after all cuts have been imposed, except for the shape χ^2 requirement. The $\pi^0\gamma\gamma$ signal reconstructs at low χ^2 , and the simulation of the $3\pi^0$ background agrees with the data above the $\pi^0\gamma\gamma$ signal. By requiring the maximum χ^2 to be less than 2.0, we are able to isolate a relatively clean sample of $K_L \rightarrow \pi^0\gamma\gamma$ events. This requirement is effective in removing fused photons separated by more than 1 cm.

Figure 4a shows the final m_{34} distribution for all events after making the photon shape χ^2 requirement. We find a total of 884 candidate events. Our simulation of the background predicts 111 ± 12 events dominated by

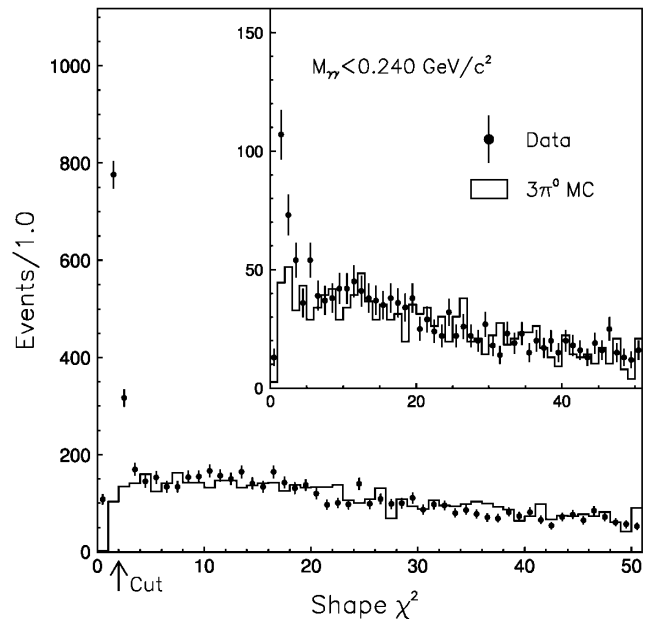


FIG. 3. The maximum shape χ^2 after all requirements, except for the shape χ^2 cut. The dots are the data and the histogram is the $3\pi^0$ Monte Carlo. The excess at low χ^2 is due to $K_L \rightarrow \pi^0\gamma\gamma$ events and the arrow indicates the position of our cut. The inset shows the same distribution for events with $m_{34} < 0.240 \text{ GeV}/c^2$, indicating the existence of a low-mass tail in $K_L \rightarrow \pi^0\gamma\gamma$ events.

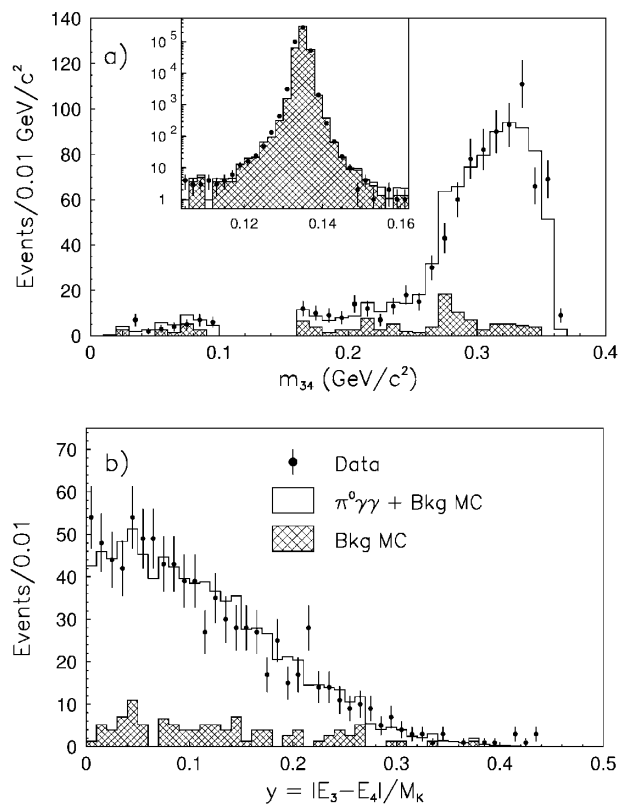


FIG. 4. (a) The m_{34} mass distribution. The $2\pi^0$ events are removed from the m_{34} distribution by cutting events between $0.10 \text{ GeV}/c^2$ and $0.16 \text{ GeV}/c^2$. The dots are the data, the histogram is the sum of the background and $K_L \rightarrow \pi^0\gamma\gamma$ Monte Carlo, and the dashed histogram is the normalized background Monte Carlo. The $K_L \rightarrow \pi^0\gamma\gamma$ MC is an $\mathcal{O}(p^6)$ calculation with $a_V = -0.7$. The inset shows the data and Monte Carlo for events in the mass region between $0.10 \text{ GeV}/c^2$ and $0.16 \text{ GeV}/c^2$ which are dominated by $K_L \rightarrow \pi^0\pi^0$ events. (b) The y parameter.

$K_L \rightarrow \pi^0\pi^0\pi^0$ events, as shown in Fig. 4a. The remaining $3\pi^0$ background is evenly divided between double and single fusion events. The level of the $3\pi^0$ background is determined by normalizing the $3\pi^0$ Monte Carlo to the shape χ^2 distribution between 5 and 20 and is consistent with absolutely normalizing the $3\pi^0$ events to the $2\pi^0$ events. In this figure, we overlay the sum of the background plus the $\mathcal{O}(p^6)$ chiral perturbation prediction for $K_L \rightarrow \pi^0\gamma\gamma$. The shapes of the data and Monte Carlo calculation match very well.

Our event sample demonstrates for the first time the existence of a low-mass tail in the m_{34} distribution. The NA31 experiment [3] had previously set a limit of $\Gamma(m_{34} < 0.240 \text{ GeV}/c^2)/\Gamma(m_{34} \text{ all}) < 0.09$. Our event sample has $73 \pm 9 \pm 9$ events above a background of $47 \pm 8 \pm 5$ events in the region $m_{34} < 0.240 \text{ GeV}/c^2$. This number corresponds to $\Gamma(m_{34} < 0.240 \text{ GeV}/c^2)/\Gamma(m_{34} \text{ all}) = 0.127 \pm 0.013 \pm 0.015$ after correcting for events that are removed by the $K_L \rightarrow \pi^0\pi^0$ cut. Figure 3 shows the maximum shape

χ^2 distribution for the events below $0.240 \text{ GeV}/c^2$, indicating an excess of events above the $3\pi^0$ background.

To extract a value for a_V , we perform a simultaneous fit to the m_{34} and y distributions. Figure 4b shows the y distribution for our final event sample. From our fit, we obtain the value $a_V = -0.72 \pm 0.05 \pm 0.06$. The systematic error is dominated by our uncertainty in the $3\pi^0$ background. We obtain a value of $a_V = -0.76 \pm 0.09$ when we fit only the y distribution. For the best fit to both distributions the χ^2 is 24.1 for 24 degrees of freedom.

To determine the $K_L \rightarrow \pi^0\gamma\gamma$ branching ratio, we normalize the $K_L \rightarrow \pi^0\gamma\gamma$ events to $K_L \rightarrow \pi^0\pi^0$ events which helps to reduce the systematic uncertainty in this measurement since we are only sensitive to differences in the relative acceptance of the two modes and not the absolute acceptance. The acceptances for $\pi^0\gamma\gamma$ and $2\pi^0$ events are 3.13% and 3.23%, respectively, for events with energies between 40 and 160 GeV and decaying from 115 to 128 m downstream of the target. Applying the same reconstruction criteria as those used in the $K_L \rightarrow \pi^0\gamma\gamma$ analysis but requiring m_{34} between 130 and 140 MeV/c^2 , we find 441 309 $K_L \rightarrow \pi^0\pi^0$ events with negligible background.

Using a Monte Carlo in which a_V is set to the best-fit value, we extract the branching ratio for $K_L \rightarrow \pi^0\gamma\gamma$ by comparing the number of $\pi^0\gamma\gamma$ events to the number of events in the normalization mode, $K_L \rightarrow \pi^0\pi^0$. Systematic uncertainties in this measurement come from the acceptance determination (2.4%), the $2\pi^0$ branching ratio (2.1%), the $3\pi^0$ background (2.1%), the a_V dependence (1.8%), the hadron veto requirement (1.8%), varying the photon shape χ^2 cut between 1 and 10 (1.8%), and the calibration (0.8%). The systematic uncertainties are added in quadrature, resulting in a total systematic uncertainty of 5.0%. We find the branching ratio to be $\text{BR}(K_L \rightarrow \pi^0\gamma\gamma) = (1.68 \pm 0.07 \pm 0.08) \times 10^{-6}$. This is consistent with the $\mathcal{O}(p^6)$ prediction [8] with $a_V = -0.72 \pm 0.06$, which is $(1.53 \pm 0.10) \times 10^{-6}$.

In summary, our measurement of $K_L \rightarrow \pi^0\gamma\gamma$ decays shows the first evidence of a low-mass tail in the m_{34} distribution. This tail is predicted by $\mathcal{O}(p^6)$ chiral perturbation theory calculations which include vector meson exchange. Our determination of a_V suggests that the CP -conserving contribution to $K_L \rightarrow \pi^0 e^+ e^-$ is between 1 and 2×10^{-12} . These contributions are approximately 2–3 orders of magnitude higher than predictions based upon the original $\mathcal{O}(p^4)$ calculations which are helicity suppressed, whereas the vector meson exchange terms present in $\mathcal{O}(p^6)$ calculations are not helicity suppressed. The contribution of the direct CP -violating amplitude to the rate for $K_L \rightarrow \pi^0 e^+ e^-$ is expected [7] to be between 1 and 4×10^{-12} .

We gratefully acknowledge the support and effort of the Fermilab staff and the technical staffs of the participating institutions for their vital contributions. We also acknowledge G. D'Ambrosio and F. Gabbiani for

useful discussions. This work was supported in part by the U.S. Department of Energy, The National Science Foundation, and The Ministry of Education and Science of Japan.

*To whom correspondence should be addressed.

Electronic address: elliott@physics.arizona.edu

†On leave from C.P.P. Marseille/C.N.R.S., France.

- [1] G. D. Barr *et al.*, Phys. Lett. B **242**, 523 (1990).
- [2] V. Papadimitriou *et al.*, Phys. Rev. D **44**, 573 (1991).
- [3] G. D. Barr *et al.*, Phys. Lett. B **284**, 440 (1992).
- [4] Particle Data Group, C. Caso *et al.*, Eur. Phys. J. C **3**, 1 (1998).
- [5] G. Ecker, A. Pich, and E. De Rafael, Phys. Lett. B **189**, 363 (1987).
- [6] A. G. Cohen, G. Ecker, and A. Pich, Phys. Lett. B **304**, 347 (1993).
- [7] J. F. Donoghue and F. Gabbiani, Phys. Rev. D **51**, 2187 (1995).
- [8] G. D'Ambrosio and J. Portoles, Nucl. Phys. **B492**, 417 (1997).
- [9] P. Heiliger and L. M. Sehgal, Phys. Rev. D **47**, 4920 (1993).
- [10] A. J. Roodman, in *Proceedings of the VII International Conference on Calorimetry* (World Scientific, Singapore, 1998).
- [11] C. Bown *et al.*, Nucl. Instrum. Methods Phys. Res., Sect. A **369**, 248 (1996).